Nanoscale Characterization of Metal/Semiconductor Nanocontacts

C. Tivarus[1], K.-B. Park[1], M.K. Hudait[2], S.A. Ringel[2] and J. P. Pelz[1]

[1]*Department of Physics, The Ohio State University, Columbus, OH*
[2]*Department of Electrical and Computer Engineering, The Ohio State University, Columbus, OH*

Abstract. Ballistic Electron Emission Microscopy (BEEM) and finite-element electrostatic modeling were used to quantify how "*small-size"* effects modify the energy barrier at metal/semiconductor nanostructure nanocontacts, formed by making Schottky contacts to cleaved edges of GaAs quantum wells (QWs). The Schottky barrier height over the QWs was found to systematically increase with decreasing QW width, by up to ~140 meV for a 1nm QW. This is mostly due to a large quantum-confinement increase (~200 meV for a 1nm QW), modified by smaller decreases due to "environmental" electric field effects. Our modeling gives excellent quantitative agreement with measurements for a wide range of QW widths when both quantum confinement and environmental electric fields are considered.

Keywords: BEEM, Schottky barrier, nanocontacts, Fermi level pinning, quantum wells, III-V semiconductors
PACS: 73.21.Fg 73.30.+y 73.63.Hs 73.63.Rt

INTRODUCTION

A number of possible near- and long-term semiconductor device technologies rely on abrupt metal/semiconductor (MS) or metal/insulator (MI) contacts with nm-dimensions, and/or with internal nm-scale inhomogeneity. It is therefore very important to develop characterization tools that can probe the *electronic* properties of buried MS and MI interfaces with sub-10 nm resolution, preferably on functional device structures. Of long-term interest are, for example, direct Schottky source/drain contacts in Si-based MOSFETs [1], or entirely new device architectures with metal contacts directly to one-dimensional structures such as carbon nanotubes or other semiconductor nanowires [1]. In the near-term, true metal films may replace poly-silicon as the gate electrode material [1], with implanted, alloyed, and/or bilayer metal films under active investigation as possible "tunable work function" metal gate materials. New metrology tools are required to characterize carrier transport through nm-dimensioned metal contacts, and/or to detect and measure the electronic effects of lateral inhomogeneities that might develop in compound materials used as source/drain or gate electrode contacts.

We are developing the technique of Ballistic Electron Emission Microscopy (BEEM) [2-6] for this important metrology need. BEEM (see Fig. 1), which is based on scanning tunneling microscopy (STM), is the only current method that allows direct measurement of a subsurface MS or MI energy barrier with nanometer-scale spatial resolution and ~15 meV energy resolution. Provided the top metal surface of a MS or MI structure of interest is accessible, a sharp STM tip can be positioned over the buried structure and be used to direct a beam of "hot" carriers towards it. In this case the hot-carrier energy and flux that can be readily controlled by adjusted by the tip bias V_T and tunnel gap d, respectively. Some of these hot carriers can surmount the energy barrier at the buried metal interface, enter the substrate, and be measured as a BEEM "collector" current I_c from the substrate. The buried structure can be imaged and the local MS or MI barrier height can be quantified by measuring how I_c depends on tip position and hot-carrier energy [2-6].

Here we present recent work where we used BEEM to directly quantify how "*small-size"* effects modify the energy barrier for carrier injection into a model metal/semiconductor nanostructure nanocontact, and used finite-element modeling to quantitatively account for the barrier modification in terms of quantum-confinement and "environmental pinning" effects. We used a model metal/semiconductor nanostructure system where the semiconductor dimension could be *systematically* varied down to ~1 nm. The model

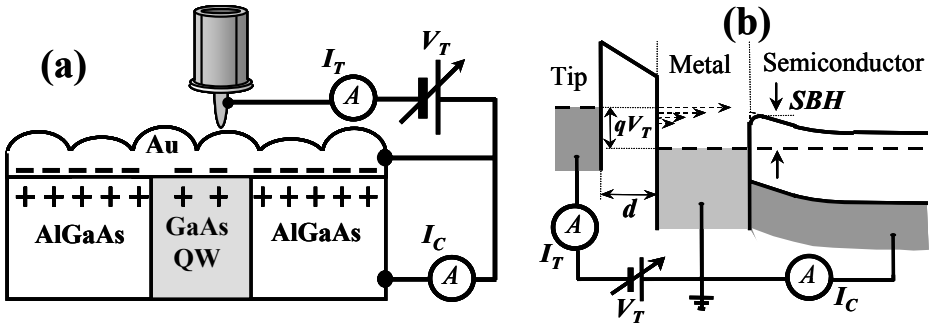

FIGURE 1. (a) Schematic diagram of sample geometry and wiring for BEEM measurements. The (+) and (-) symbols represent positive interface state charge negative image charge, respectively. (b) Corresponding energy-level diagram.

system is an Au Schottky contact formed on a cleaved GaAs/AlGaAs heterostructure containing a series of GaAs quantum-wells (QWs) of different width (see Fig. 1(a)).

Since the local Schottky barrier height (SBH) over the cleaved QWs is lower than over the surrounding AlGaAs regions, we can locate the QWs by looking for regions of enhanced BEEM current, and then directly measure the local SBH for each individual QW to determine how the SBH depends on the QW width *d*. Some of this work was initially presented elsewhere [6].

Experiments

Our samples were Schottky diodes made on the cleaved side of a heterostructure grown by molecular beam epitaxy (MBE) consisting of a sequence of GaAs QWs (~5×10^{16} cm^{-3} n-type) with width varying between 1 nm and 15 nm, separated by 200 nm-thick $Al_{0.3}Ga_{0.7}As$ barrier layers (~1×10^{17} cm^{-3} n-type) on top of an n-type (~3×10^{17} cm^{-3}) GaAs(001) substrate. The wafers were cleaved *ex-situ* along a [110] direction and ~300 μm diameter Au dots were made using photolithography or evaporation through a shadow mask. Gold metal layers with thickness of 4 nm and 7 nm were evaporated using e-beam or thermal evaporation at a typical pressure of $2x10^{-7}$ torr. Samples were then transferred into an ultra high vacuum Omicron VT STM system which was custom-modified for BEEM measurements.

Figure 2(a) shows a 400 x 200 nm STM topographic image of the top Au film surface of a sample, while Fig. 2(b) shows the *simultaneously* measured BEEM image revealing where 7 nm (left) and 9 nm (right) wide cleaved QWs intersect the buried Au interface.

The granular structure in the topography is due to the polycrystalline grains in the Au film. The bright stripes in Fig. 2(b) (over the QWs) are regions with enhanced BEEM current due to the lower local SBH [4, 6]. Once the QWs were identified, the STM tip was positioned over a particular QW, and a local "BEEM spectrum" was measured by ramping the tip bias V_T to measure how the BEEM current varies with V_T. These spectra (not shown here) are characterized by a *BEEM threshold voltage* V_{thresh} [5] above which hot carriers have sufficient energy to surmount the buried Schottky barrier, enter the substrate, and be measured. The local SBH is then directly given as qV_{thresh} , where q is the elementary charge.

The data points (triangles) in Fig. 3 show how the measured SBH over a particular QW depends on the QW width *d*. We see that the SBH *increases systematically by* ~140 meV *as the QW width d is reduced from 15 to 1 nm*. For reference, the lower

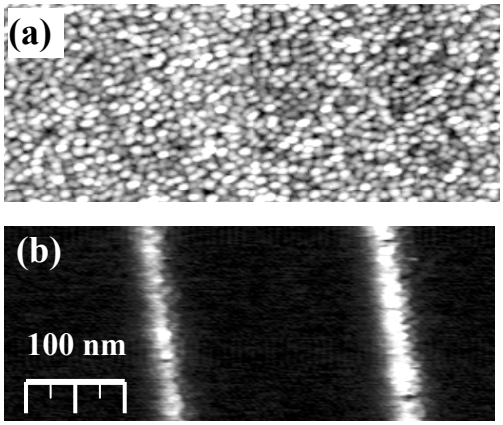

FIGURE 2. (a) STM image of the top 7 nm thick Au film over 7 nm (left) and 9 nm (right) QWs, and (b) simultaneous BEEM image of same area. The subsurface QWs are only visible in (b). Grey scale: 4.6 nm for (a), 0-4 pA for (b). All data taken with V_T = 1.15 V and I_T = 15 nA.

dashed line (at ~0.90 eV) in Fig. 3 is the SBH measured over wide GaAs reference layers, while the upper dashed line (at ~1.085 eV) is the SBH measured over the AlGaAs barrier layers. As discussed below, "*small-size"* effects produce this strong increase in the energy barrier that carriers must surmount in order to enter the QWs. They are similar to the small size effects that are expected to exist in any metal contact to any semiconducting nanostructure.

Discussion and Modeling

In order for electrons to enter a semiconducting nanostructure (the QWs in this case) they must find available conducting states in the nanostructure conduction band. In general, two size-related factors can alter the energy of these propagating states. (1) the most obvious effect is *quantum confinement*, which increases the minimum energy that a carrier must have to propagate in the nanostructure. This energy increase is relative to the conduction band minimum (CBM) of the material the nanostructure is made from. (2) Less obvious are the effects of "non-local" or *environmental* electric fields, due an *inhomogeneous charge distribution* in and around the nanostructure [7-9]. These environmental electric fields can shift the potential energy of a carrier as it enters or exits a nanostructure, and hence shift the conduction band energy in the nanostructure relative to its value in an uniform material. It is important to understand that these are different effects: environmental electric fields shift the conduction band, while quantum confinement increases the minimum energy of propagating states relative to this (shifted) conduction band minimum. Below we consider these two effects separately, and then compare their combined effects to the measured change to the SBH as the QWs are made narrower.

In order to estimate the effect of quantum confinement, we used a simple one-dimensional (1D). We note that this neglects the fact that the QW is in fact not infinitely long, and that there exists a fairly strong depletion field (~2×10^5 V/cm) near the QW opening. The dashed line in Fig. 3 shows the calculated SBH from this simple 1D model, using literature values for the GaAs effective mass $m^* \cong 0.067\ m_0$, the surrounding $Al_{0.3}Ga_{0.7}As$ barrier layer $m^* \cong 0.092\ m_0$ [10] (where m_0 is the free electron mass) and for the conduction band offset $\Delta E_{CB} \cong 0.250$ eV between the GaAs QW and the $Al_{0.3}Ga_{0.7}As$ barriers [11]. We see that even this simple 1D quantum-confinement model describes the measured data fairly well, although it systematically overestimates the actual increase in SBH. This demonstrates that quantum-confinement effects are very strong at these dimensions, and can be directly measured using BEEM.

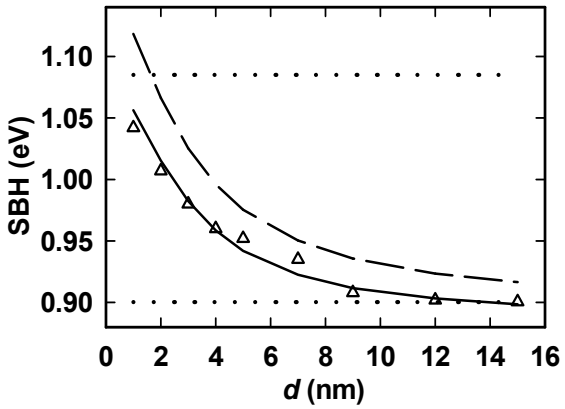

FIGURE 3. Schottky barrier height as a function of QW width d: experimental data (empty triangles), simple 1D model (dashed line), full model (solid line).

We next consider the expected effects of environmental electric fields. It has long been known that *interface state charge* near a MS interface can produce an electric dipole layer, which can shift the energy of the conduction band minimum (and hence the SBH) at the MS interface. For uniform system this shift is easy to calculate in terms of the parameters that describe the interface states, and has long been used to describe Schottky barrier "pinning" at MS interfaces [12]. Recently several authors have considered the effects of *spatially inhomogeneous interface states* that may exist at MS nanocontacts [7-9]. Here we consider three possible effects. (i) It has been argued that pinning can be *weakened* if the area of the nanocontact is very small, simply due to the small total amount of interface charge at the nanocontact [7,8]. This results in a shift of the conduction band closer to the expected energy if interface states did not exist. (ii) An abrupt local variation in interface charge can produce a so-called "lightning rod effect," *i.e.* strong geometry-induced local electric fields. This can change the well-known "image force lowering" of the SBH,

$$\Delta SBH_{IFL} = -q\sqrt{qE_d / 4\pi\varepsilon_r\varepsilon_0} \quad (1)$$

that occurs whenever there is an electric field E_d at the metal interface [12]. (iii) A strong local electric field produces large local band-bending. This can produce a *physically thinner* Schottky barrier at the nanocontact, which can allow greatly increased tunneling *through* the Schottky barrier [9]. Here we only consider the effects of (i) and (ii), since our measurements and

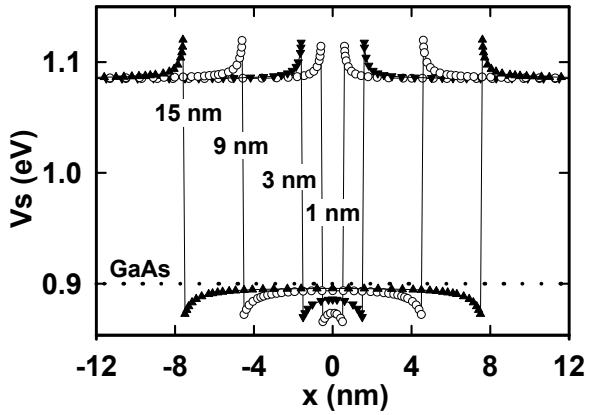

FIGURE 4. Calculated conduction band minimum along a line parallel to the interface, at a depth just under the interfacial layer. For reference, the dotted line shows the conduction band minimum for a *uniform* Au/GaAs interface.

modeling mainly concern the *height* of the energy barrier at the QW opening.

To estimate these two effects, we have calculated the potential distribution near the Au/semiconductor interface close to a QW using the FLEXPDE finite-element solver [13]. The model geometry and coordinate system is illustrated in figure 1(a). As discussed above, interface charge (shown as "+" symbols in Fig. 1(a)) and its image charge in the metal film (shown as "-" symbols) produce a potential drop across a thin "interfacial layer" at the metal/SC interface, thus altering the effective Schottky barrier height [12].

We note here that the values of the relevant interface parameters for Au/GaAs and Au/AlGaAs are not universally agreed upon, so we did our modeling using a physically reasonable set of parameter vaules that give the measured SBH and interface pinning strength for *uniform* Au/GaAs or $Au/Al_{0.3}Ga_{0.7}As$ interfaces. As we see below, the calculated shift to the SBH from these effects is actually rather small. As a check, we also considered other parameter values found in the literature (but in combinations that still produce the measured SBH and pinning strength for uniform interfaces), and in general found very similar reduction (within 5-15 meV) in the calculated GaAs CBM for the different QW widths. For GaAs, the assumed parameters are: charge neutrality level CNL = 0.53 eV above the valence band maximum (VBM), interface states density $D_s = 1.25 \times 10^{18}/m^2$, electron affinity $\chi = 4.07$ eV and relative dielectric constant $\varepsilon_r = 13.1$ [12]. For $Al_{0.3}Ga_{0.7}As$: CNL = 0.70 eV above the VBM [14], $D_s = 2.65 \times 10^{18}/m^2$, $\chi = 3.74$ eV and $\varepsilon_r = 12.2$ [15]. The bandgap for GaAs and $Al_{0.3}Ga_{0.7}As$ was taken to be 1.423 eV and 1.845 eV respectively [10], and Au work function was taken to be 5.1 eV [12]. We also assume a 0.4 nm thick interfacial layer with a dielectric constant equal to the free space value [12].

Figure 4 shows the calculated CBM for several different QW widths, along the direction parallel to the interface at a depth just under the interfacial layer. Compared with the Au/ reference GaAs (dotted line), we see that environmental pinning from the neighboring $Au/Al_{0.3}Ga_{0.7}As$ interface *reduces* the conduction band minimum in the QW, with the strongest reduction close to the GaAs/AlGaAs interface. Physically, the positive interface charge is larger on the surrounding metal/$Al_{0.3}Ga_{0.7}As$ interface than on the metal/QW interface, as illustrated in Fig. 1(a)). This stronger "environmental" positive charge produces a stronger electric field across the QW interfacial layer than would exist for a uniform Au/GaAs interface, with a corresponding greater reduction in the GaAs bulk CBM. The calculated reduction is not large, ranging from ~5 meV for $d = 15$ nm to ~30 meV for $d = 1$ nm.

Figure 5 shows the calculated potential profile perpendicular to the Au interface along the center of a QW for several different values of d. Also included in Fig. 5 is the potential profile corresponding to a uniform Au/GaAs Schottky barrier.

We see that the near-interface electric field is stronger for the QWs as compared with bulk GaAs and is strongest for the narrowest QWs. There are two factors that contribute to this stronger electric field. First, the larger SBH of the $Au/Al_{0.3}Ga_{0.7}As$ SB results in a larger depletion width (and hence a stronger

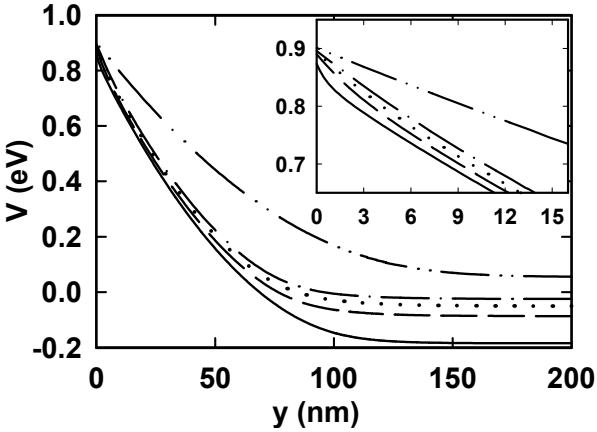

FIGURE 5. Potential profile along center of QW for: uniform Au/GaAs (dot-dot-dashed), 15 nm QW (dot-dashed), 9 nm QW (doted), 5 nm QW (dashed) and 1 nm QW (solid). Inset: zoom-in close to the semiconductor surface. Zero potential corresponds to the $Al_{0.3}Ga_{0.7}As$ Fermi level position.

depletion field) than for a uniform metal/GaAs SB. A GaAs QW embedded in this larger depletion region will "feel" the stronger depletion field, provided the QW width is smaller than the $Au/Al_{0.3}Ga_{0.7}As$ depletion width. In addition, the "environmental" local charge distribution further enhances the local electric field over the QWs, with the strongest enhancement for the narrower QWs. This increased electric field for the QWs as compared to a uniform metal/GaAs SB results in a *slightly increased image force lowering* as given in Eq. (1). Note that an *increased lowering* means a lower local SBH over the QWs. In our case, the image force lowering turns out to be $\Delta SBH_{IFL} \cong 35$ meV for a uniform Au/GaAs interface, $\cong 47$ meV for a 15 nm QW, and $\cong 69$ meV for a 1 nm QW. Hence the "extra" lowering of the SBH due the image force ranges from (47 meV – 35 meV) $\cong$ 12 meV for a 15 nm QW to $\cong$ 34 meV for a 1 nm QW.

We can now compare with the measured data. The solid line in Fig. 3 shows the sum of (i) the estimated (large) increase in SBH due to simple 1D quantum confinement, (ii) the (small) reduction in the SBH due to reduced pinning over the QWs, and (iii) the (small) reduction in the SBH due to image force lowering. The overall agreement between this refined model and the data is very good, indicating that we have accounted for all the relevant small-size effects in this model metal/nanostructure system.

Conclusions

In summary, we have used Ballistic Electron Emission Microscopy and finite-element modeling to directly quantify and analyze the influence of "*small-size"* effects on carrier transport through a metal/QW nanocontact system. The local Schottky barrier shows a strong (~140 meV) increase as the QW width is reduced to $d = 1$ nm. This is due to a strong increase in the quantum confinement energy (up to ~200 meV for d = 1nm), modified by smaller decreases to the Schottky barrier height due to environmental pinning and image force effects. Excellent quantitative agreement over the full range of QW widths is obtained when both quantum confinement and environmental electric field effects are considered. We note that it should be possible to use BEEM to make similar nm-resolution measurements on other metal-semiconductor and metal-insulator systems, provided the top metal film is thin (<~10 nm) and accessible to an STM tip. We expect that these small-size effects can be much stronger for metal nanocontacts to 1D semiconductor nanowires, and so must be characterized and understood for possible future electronic devices based on such nanowires.

This work was supported by the Semiconductor Research Corporation, the National Science Foundation, and the Office of Naval Research.

References

1. International Technology Roadmap for Semiconductors, 2003 Ed (available at http://public.itrs.net/).
2. B. Kaczer, H.-J. Im, J.P. Pelz, and R. M. Wallace, Appl. Phys. Lett. **73**, 1871 (1998).
3. H.-J. Im, B. Kaczer, J. P. Pelz, and W. J. Choyke, Appl. Phys. Lett. **72**, 839 (1998).
4. Y. Ding, K.-B. Park, J. P. Pelz, K. C. Palle, M. K. Mikhov, B. J. Skromme, H. Meidia and S. Mahajan**,** Phys. Rev. B **69**, 041305 (2004).
5. W.J. Kaiser and L.D. Bell, Phys. Rev. Lett. **60**, 1406 (1988); **61**, 2368 (1988).
6. C.Tivarus, M.K. Hudait, S.A. Ringel, J.P. Pelz, *accepted for publication in Phys. Rev. Lett*., 2005.
7. F. Leonard and J. Tersoff, Phys. Rev. Lett**. 84**, 4693 (2000).
8. H. Hasegawa, T. Sato and C. Kaneshiro, J. Vac. Sci. Technol. B 7, 1895 (1999).
9. G.D.J. Smit, S. Rogge and T.M. Klapwijk, Appl. Phys. Lett. **80**, 2568 (2002); Microelec. Eng. **64**, 429 (2002).
10. P. Roblin and H. Rohdin, *High–speed heterostructure devices*, (Cambridge Univ. Press 2002).
11 J.J. O'Shea, E.G. Brazel, M.E. Rubin, S. Bhargave, M.A. Chin, V. Narayanamurti, Phys. Rev. B **56**, 2026 (1997)
12. S.M. Sze, *Physics of semiconductor devices* (John Wiley & Sons, Inc. 1969).
13. www.pdesolutions.com.
14. R.E. Allen, T.J. Humphreys and J.D. Dow, Solid State Commun. **49**, 1 (1983).
15. L.D. Bell, Phys. Rev. Lett**. 77**, 3893 (1996).